most behavioral functions appear to be relegated not to single cells but to groups [5]. Thus, regarding the group as a unit may have special merit. In this connection, Wu et al.'s paper describes methods for analyzing multicellular activity using voltage sensitive dyes; and Camhi describes a multicellular code for stimulus direction.

Concerning the third partial goal, determining the functional properties of the system's components, which properties does one want to analyze? Speaking of a single neuron, it has been learned in recent years that these come with a rich variety of properties. There are cells, probably the majority, that support all-or-none action potentials, and others that do not use action potentials at all. There are cells whose output directly reflects their synaptic input, and others whose membranes are capable of generating rhythmic oscillations or prolonged plateau potentials. Indeed, the number of known types of membrane channel, each producing a different variety of voltage signal across the neuronal plasma membrane, has grown enormously in recent years. A proper analysis of a cell as a circuit element is thus a deeply complex affair. Moreover, the physiological properties of the cell are subject to neuromodulatory variation, as the paper by Selverston points out.

As to the fourth partial goal, analyzing the interactions among components, again numerous complexities of synaptic interactions have been described in recent years. Aside from the classic distinctions; electrical vs chemical, excitatory vs inhibitory, functionally strong vs weak, facilitating vs nonfacilitating or antifacilitating synapses, we now have as well synapses with a variety of types of conductance change, those with short-term or long-term modifiability, and those using first and/or second chemical messengers. Again, the analysis at this level is highly complex.

The fifth partial goal, reconstructing a behavior on the basis of its known components and their interactions, has rarely been achieved. Partial attempts are seen in several of the papers of this collection.

It is fair to say that no single example of behavior has been fully analyzed with regard to all five of the partial goals mentioned above. But the fact is that there is yet a sixth partial goal that must be mentioned. For as ethologically oriented scientists, we must try to understand how the animal's nervous system solves the problems it encounters under real field conditions. And even beyond this, one would want to know how the solution to these problems has developed since the animal's a birth, and has evolved through time.

The papers in this collection provide, then, partial insights into the overall problem of understanding the neural basis of natural behavior. It is hoped that by 'connecting the dots' between these contributions, the reader will be able both to see the whole sweep of the field of neuroethology, and to recognize vast and exciting areas ripe for investigation.

The papers are sequenced in a 'bottom up' order, beginning with subcellular analysis, then on to network studies, and onward to the whole animal in the field. I am delighted that a true grand master of invertebrate neuroethology, Franz Huber, has provided us with an epilog that offers wise guidance for the future development of our discipline.

Acknowledgments. I thank Dr R. Goldstein for kindly reviewing this introduction.

1 Camhi, J. M., Neuroethology: Nerve Cells and the Natural Behavior of Animals. Sinauer, Sunderland, Massachusetts 1984.
2 Ewert, J.-P., Neuroethology: An Introduction to the Neurophysiological Fundamentals of Behavior. Springer-Verlag, Berlin 1980.
3 Ewert, J.-P., Capranica, R. R., and Ingle, D. S. (Eds), Advances in Vertebrate Neuroethology. Plenum Press, New York 1983.
4 Huber, F., and Markl, H., Neuroethology and Behavioral Physiology: Roots and Growing Points. Springer-Verlag, Berlin 1983.
5 Kupferman, I., and Weiss, K. R., The command neuron concept. Behav. Brain Sci. *1* (1978) 3–40.

0014-4754/88/050361-02$1.50 + 0.20/0

Analysis of synaptic integration using the laser photoinactivation technique

G. A. Jacobs and J. P. Miller

Dept. of Zoology, University of California, Berkeley (California 94720, USA)

Summary. Crickets (and many other insects) have two antenna-like appendages at the rear of their abdomen, each of which is covered with hundreds of 'filiform' hairs resembling the bristles on a bottle brush. Deflection of these filiform hairs by wind currents activates mechanosensory neurons at the base of the hairs. The axons from these sensory neurons project into the terminal abdominal ganglion to form a topographic representation (or "map") containing information about the direction, velocity and acceleration of wind currents around the animal. Information is extracted from this map by primary sensory interneurons that are also located within the terminal abdominal ganglion. In this paper, we review the progress that has been made toward understanding the mechanisms underlying directional sensitivity of an identified sensory interneuron in the cricket, *Acheta domesticus*. The response properties of the cell have been found to depend to a large extent upon the structure of its dendritic branches, which determines its synaptic connectivity with the sensory afferents in the map of wind space and the relative efficacy of its different synaptic inputs.

Key words. Cricket; cercal sensory system; mechanosensory interneuron; photoinactivation.

Introduction

It has been a long-term goal of many neuroscientists to determine how information is processed in central nervous systems. A great many researchers have focused their attention upon information processing in sensory systems. One general principle that has emerged from studies of the structure and function of sensory systems is that the 'relevant properties' of sensory stimuli are often represented within computational maps. As defined in a recent review [13], a map is an array of neurons through which there is a systematic variation in the 'tuning' of neighboring neurons for a particular parameter. The representations of retinal coordinates on the tectum and higher visual areas are familiar examples of topographic sensory maps, in which the mapped parameter is the location of an object in visual space. A 'computational map'

is a map in which the representation of sensory information is transformed into a place coded probability distribution that represents the computed values of parameters by sites of maximum relative activity [13]. Familiar examples of computational maps include the representation of line orientation within 'hypercolumns' of the mammalian visual cortex [5, 6] and the representation of inter-aural delay in the nucleus laminaris of the barn owl [14].

We are interested in the cellular mechanisms by which information is extracted from such a topographically organized sensory map. We have concentrated our efforts on studying primary sensory interneurons, whose function it is to 'read' and 'interpret' information from such maps [1, 7, 8]. The system we are studying is the cricket cercal sensory system which is an excellent example of this type of anatomical organization. It is a complex mechanosensory system which subserves at least three different sensory functions: wind [1, 3, 7, 8, 10, 11, 18, 23, 30], touch [22] and gravity [21, 25] sensitivity. The primary afferents for these three modalities form three separate sensory maps in the terminal abdominal ganglion [1, 2, 22, 32]. There are three sets of interneurons that subserve these different modalities, and in most cases the modality of a particular interneuron can be predicted based on the location of its dendritic field [1, 8, 10, 22, 25].

The modality in which we have been the most interested is wind direction sensitivity, mediated by filiform afferents and directionally selective sensory interneurons. Crickets bear two large sensory appendages called cerci at the tip of the abdomen. Each cercus is covered with approximately 1000 filiform hairs and each hair is innervated by a single sensory neuron [1, 4]. The structure of a cuticular 'hinge' at the base of each hair constrains motion to a single plane [4]. When the hair is displaced in one direction in one plane, the sensory neuron fires action potentials. In the 'return' direction, no spikes are generated. The thousand-or-so hairs on each cercus are arranged in many different orientations, insuring that several hairs will be displaced for any possible wind stimulus in the horizontal plane. As well as depending on the direction of wind stimuli, the response properties of the mechanosensory cells also depend upon the velocity and acceleration of the wind currents.

The axons of all the filiform mechanosensory receptors project into the terminal abdominal ganglion, and arborize within two bilaterally symmetrical regions called the 'cercal glomeruli' [1, 32]. Bacon and Murphey [1] have determined that the afferent endings form a topographic 'map' of their locations on the cercus within the glomeruli. Since the directional sensitivity of each of the filiform hairs is correlated with its location on the cerci, a consequence of the topographic projection is that a 'map' of wind direction is set up in the cercal glomeruli. In other words, within any one restricted region in a glomerulus, the synaptic endings from filiform afferents can only be activated by wind stimuli that have a vectorial component along a particular direction with respect to the animal's body. The optimal wind stimulus orientation varies systematically throughout the volume of the glomerulus.

Although the representation of wind direction within this map is fairly well understood, it is not known how the information concerning wind velocity and acceleration is represented within the glomeruli. Certainly, there is no apparent anatomical correlate of stripe-like 'nesting' of different maps, such as the ocular dominance columns in the optic cortex. It is therefore likely that each region of the direction map is permeated by synaptic terminals from afferents having the full range of velocity and acceleration characteristics.

The cells which carry information about wind direction and velocity out of the ganglion to higher centers are pairs of primary sensory interneurons [1, 3, 10, 11, 18, 27, 30]. At least 10 different interneuron pairs have been identified [10, 18] and the directionally selective response properties of several of these cells have been investigated [1, 7, 8, 17, 30]. Mechanisms underlying directional sensitivity in some of these cells have been studied in great detail [7, 8, 16]. Their directional sensitivities have been shown to be directly related to the position of their dendrites within the topographic map of wind direction formed by the filiform afferents discussed above [1, 8]. Identified interneurons with different morphologies have very different directional sensitivities (Bacon [2]; and Miller and Jacobs, unpublished observations). A detailed analysis of how one of these interneurons, neuron 10-3, extracts information concerning the direction of wind stimuli from the map was the subject of the studies reviewed below.

Our working hypothesis first proposed by Bacon and Murphey [2] was that these interneurons derived directional sensitivity to wind stimuli by virtue of the position of their dendrites within the map of wind direction. Each interneuron has between one and four major dendritic branches, and each branch is located in a different region of the topographic map. Since each dendrite should receive input from a class of afferents sensitive to a different wind direction, the cell as a whole should be sensitive to the sum of those wind directions. This sum would then comprise the 'excitatory receptive field' of the neuron. Bacon and Murphey's studies [1] demonstrated a good correlation between receptive field organization and dendritic structure. Our experiments were designed to examine this structure/function relationship in detail, to understand how inputs distributed throughout the dendritic tree of an interneuron were integrated into a directionally selective spiking output [7, 8, 19]. We found that this structure/function relationship was much more complex than had been previously stated. These interneurons receive, in addition to excitatory inputs from afferents, polysynaptic inhibitory inputs which significantly affect the precise tuning of their directional selectivities [8, 9, 15, 16]. We also found that particular excitatory inputs to certain dendrites were more efficacious than others in controlling the spiking output of the cell [8].

These studies were made possible through the use of a new technique, developed over the last few years in this laboratory. The technique involves the use of a laser to perform precise lesions of single dendritic branches, using dye sensitized photoinactivation [7, 8, 20]. Since much of the structure/function analysis depended on being able to reveal the functional characteristics of different regions of the neuron, the laser photoinactivation was invaluable in this respect. In this review we will first summarize the experimental apparatus and protocols used in these studies, and then discuss what we have learned through applications of these techniques.

Laser photoinactivation technique

When a neuron is filled with a fluorescent dye and illuminated with intense light of the appropriate wavelength, the cell becomes functionally inactivated [20]. It is neither the dye nor the illumination alone that harms the tissue, but an interaction of the light *and* the dye that produces the damage. The light activates the dye to catalyze a reaction which produces 'singlet' oxygen: a very reactive form which causes oxidative damage to functional regions of enzymes and ion channels [29]. This technique has been used very successfully to eliminate cells from circuits in vivo, and to reduce the complexity of circuits to aid in understanding the basis of central pattern generation in the lobster stomatogastric system (for review see Selverston and Moulins [26]).

We have recently refined this technique to allow functional inactivation of parts of single cells. This is accomplished by filling the whole neuron with dye, but illuminating only a small portion of the cell with light intense enough to cause photooxidative damage. The apparatus for producing the small diameter, 'targetable' beam include a commercially

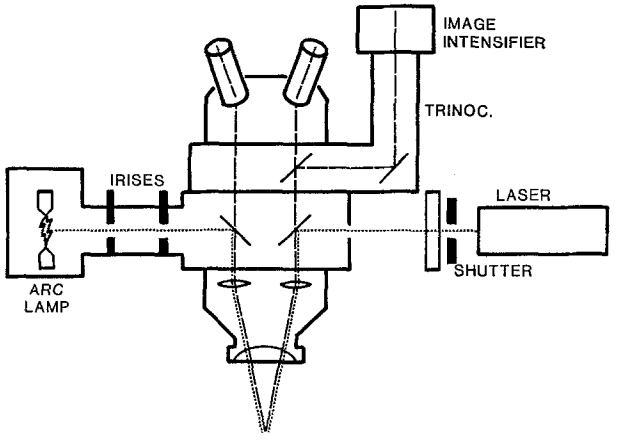

Figure 1. Schematic diagram of laser photoinactivator apparatus. The preparation is viewed through a stereo-dissecting microscope (Wild M5-Apo). An epifluorescence attachment allows the operator to illuminate the tissue with a mercury arc lamp and/or a laser (Liconix HeCd 4210). Fluorescence of the sample at low light levels is viewed directly with a microchannel plate image intensifier (ITT #MX9644/UV) connected to a trinocular attachment. Adapted from Kater et al.[12].

available dissecting microscope with epifluorescence and trinocular attachments, a microchannel plate image intensifier, a laser, and a movable optical bench (fig. 1).

A stereo dissecting microscope was needed for these studies, due to the large working distance required for placement of electrodes and the wind stimulus generator. In order to achieve a beam with high enough intensity and small enough diameter, we decided to utilize a laser, and to direct the laser beam down through one beam path of the stereo microscope using an epifluorescence attachment. The laser beam characteristics are controlled by a variable attenuator, a beam contractor, and an electronic shutter. The beam is directed into the epifluorescence attachment using a series of front-surfaced mirrors. Due to the high quality of the microscope optics, we were able to achieve a beam diameter at the tissue of 30 μm, which is optimal for the ablation of single dendritic branches.

Since the microscope objective serves as the final condensing stage for the laser beam, the target location for photoinactivation was selected by moving the microscope with respect to the tissue. The laser beam always maintains the same location in the microscope's field of view. Movement of the microscope was achieved by attaching the apparatus to three orthogonally-mounted, linear translation stages, each of which was driven with a DC stepper motor. Two stages move the microscope in the horizontal plane, and the third stage serves as the focus control. In order to visualize the neuron for purposes of aiming of the laser beam, a second light source was used. This was a 100-W Mercury Arc lamp, also mounted to the epifluorescence attachment, and set up to direct its light through the beam path not being used for the laser. Since illumination of the dye-filled cells with the full intensity of this mercury arc lamp would itself cause photooxidative damage, the intensity of this light was kept well below the threshold for any observable effects during the laser targeting. In practical terms, this means that the intensity must be kept below the level required to cause any visible fluorescence. This necessitates the use of an image intensifier, connected to a trinocular attachment above the epiillumination stage. This compact, solid state device forms an image of the dye-filled cell on a 25-mm-diameter phosphor screen with a luminance gain of about 80,000. Also visible on the screen was an image of a cross hair reticule, indicating the location in the visual field at which the laser beam is targeted when the electronic laser shutter is opened. To aim the beam, the operator monitors the image intensifier with the arc lamp on and the laser beam off, and translates the microscope apparatus in three dimensions until the cross hairs are centered over the dendrite to be inactivated. For a detailed list of all components used in construction of this apparatus, see Kater et al.[12].

The application of the technique can best be described by narration of the procedures during a typical experiment. First, the experimenter achieves an intracellular penetration of a test cell, using an electrode filled with Lucifer Yellow or 6-carboxyfluorescein. The cell is then filled with the dye by iontophoresis (typical parameters: − 3 nA for 10 min). The input resistance and resting potential of the cell are recorded as control measurements of the cell's overall viability. The apparatus is moved so that the laser beam will illuminate the cell at the particular site of interest. The laser shutter is then opened for a period ranging from 3 to 15 s. Immediately following the illumination, the section of neurite receiving direct illumination was usually bleached. There was an initial decrease in input resistance, followed by a steady increase in input resistance. Our criteria for a successful transection were 1) stabilization of the resting potential to within 5% of the preillumination value and 2) recovery of the input resistance to a value equal to or greater than the pre-illumination value by 15 min after the laser illumination. Note that the closer the target site is to the recording site, the greater will be the apparent increase in input resistance, since a greater amount of the 'local' membrane has been isolated from the recording electrode.

This technique has now been successfully applied in crickets[7,8] and rat hippocampal pyramidal cells (Malinow and Miller, in review). We note that the technique has not been successful in the CNS of lobster and crayfish (unpublished observations). The applicability of this technique probably depends upon several biochemical and metabolic properties of the particular cell type, including the level of endogenous activity of superoxide dismutase systems.

The cricket cercal afferent system

How is the information about wind direction extracted from the topographic map of wind sensitive afferents? Many of the interneurons have individual dendrites located in different neuropil regions that encode different wind directions[1,10]. We are interested in how the structure of these cells results in a directionally selective output specific to each cell. We have concentrated on one of these interneurons, 10-3, shown in figure 2. This interneuron has three different dendrites, designated with the letters X, Y, and Z that are located in three non-overlapping regions of the terminal ganglion[8]. Each dendrite occupies a region of neuropil populated by afferents activated by different wind directions. These anatomical data suggested that the receptive field of the cell should be composed of the sum of these excitatory inputs to each of its dendrites.

As a first step in the structure/function analysis of this cell the directional sensitivity of the cell was measured to determine whether the anatomical predictions of the excitatory receptive field were valid. Responses of the interneuron to constant velocity wind stimuli delivered at different positions around the animals body in the horizontal plane were recorded.

The directional sensitivity of interneuron 10-3 to such stimuli is shown in figure 3. The responses were measured in two ways: 1) the area under the waveform during each wind stimulus was calculated, and 2) the number of spikes generated during each wind stimulus were counted. These data were scaled to the maximum response, and plotted in both linear and polar coordinates (fig. 3). The polar plot illustrates the

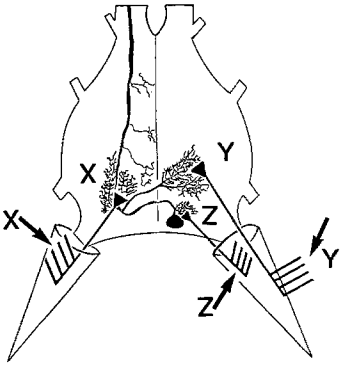

Figure 2. Interneuron 10–3 and its excitatory synaptic inputs from filiform mechanosensory cells. Interneuron 10–3 has three distinct dendritic branches, each located in a different region of the terminal abdominal ganglion. Each branch on this camera lucida drawing has been labeled with a different letter: X, Y, or Z. The three classes of afferents thought to provide input are represented on the schematic diagram of the cerci, shown here as cones at the posterior end of the outline of the terminal ganglion. The wind directions with respect to the animal's body that activate each set of afferents are represented with arrows. Reprinted with permission from Science *228* (1985) 344–346.

cell's directional sensitivity with respect to the animal's body. For the linear plot, the maximum response was plotted in the center to illustrate the sharpness of the cell's directional tuning. The results demonstrate that the interneuron was maximally sensitive to wind from the front left side of the animal's body, as would be predicted by the dendritic anatomy. By observing the movements of particular hair classes on the cerci during the wind stimuli, we could correlate the recorded response in the cell with the activation of inputs to different dendrites. The maximal responses in 10–3 occurred at positions that activate inputs to dendrites X and Z. At positions that activate dendrite Y alone, (i.e., wind directed from the front right side of the animal's body) the cell fired at a much lower frequency. These response properties of the interneuron fit the anatomical predictions for the excitatory receptive field quite well.

In addition to receiving the predicted excitatory inputs, the interneuron received inhibitory inputs at approximately half the wind positions tested. Previous results suggest that inhibitory inputs are mediated polysynaptically by unidentified inhibitory interneurons. The inhibitory inputs were manifest in two ways: either 1) by a hyperpolarization of the membrane potential or 2) by the apparent shunt of action potentials which would normally be produced by the wind stimuli.

The results of these experiments clearly indicated that the cellular mechanisms underlying directional selectivity were far more complex than a simple summation of excitatory inputs from filiform afferents. Three different factors must be considered to account for the observed response properties of the cell: 1) the receptive fields of individual dendrites, 2) the inhibitory 'surround' and 3) the relative strengths of excitatory and inhibitory inputs at the spike initiating zone. To simplify our analysis we used the laser photoinactivation technique to determine the functional properties of individual dendrites.

Response properties of individual dendrites

One of the underlying assumptions about the excitatory inputs to interneuron 10–3 is that since each dendrite occupies a different region of the map of wind direction, each dendrite should have its own receptive field and directional selectivity. There are two ways to test this hypothesis using the laser photoinactivation technique. One way is to isolate a single dendrite and measure its receptive field. The other is to ablate a dendrite and measure the residual receptive field of the remainder of the cell. These two experiments were performed on interneuron 10–3 and the results are shown in figure 4. To isolate a single dendrite, the laser was targeted at the neurite midway between dendrite Z and dendrite X. Under these circumstances, the cell was reduced to the soma plus dendrite Z. Prior to photoinactivation, the cell was most sensitive to wind aimed at the anterior and left side of the animal's body. After the inactivation, the maximal sensitivity shifted approximately 60° toward the left rear of the animal. The maximum response was then obtained at positions which corresponded to wind directed at the medial face of the right cercus. According to the anatomical map of afferent projections, this position is the optimal stimulus orientation for afferents that overlap with dendrite Z. The directional sensitivity which was measured therefore represents the receptive field of dendrite Z. This experiment also revealed two other pieces of information: 1) inhibitory inputs recorded before photoinactivation were not observed after dendrite Z was isolated, and 2) no action potentials were recorded following the isolation, which suggests that spike initiating zone and active membrane are located somewhere beyond the point of ablation.

In a complementary set of experiments, dendrite Y was removed from the neuron by targeting the laser beam midway along the neurite which connects this dendrite to the rest of the cell. The results of one such experiment are shown in figure 4. In this experiment, dendrite Y was ablated in a preparation in which the left cercus (contralateral to 10–3's

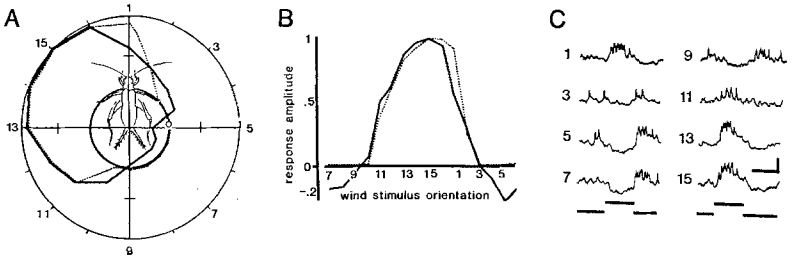

Figure 3. Directional sensitivity of interneuron 10–3. A polar plot of wind-evoked responses. The outer circle represents the amplitude of the maximum response recorded from this cell, to which all other responses were scaled. The inner circle represents the baseline or zero-level activity. The numbers and tics around the outer circle indicate the 16 wind orientations at which test responses were evoked. The solid curve plots the area under the compound postsynaptic potential evoked by the wind stimuli (a value within the inner circle represents a hyperpolarization from the resting level). The dashed curve plots the number of action potentials evoked by the wind stimuli. *B* The same data as is plotted in A, but is replotted in rectilinear coordinates starting at position 7 and proceeding clockwise around the polar plot. *C* Examples of the recordings from which the data for plots A and B were measured. The bottom traces indicate the duration of the constant velocity wind stimuli. Scale bars: 200 ms, 5 mV.

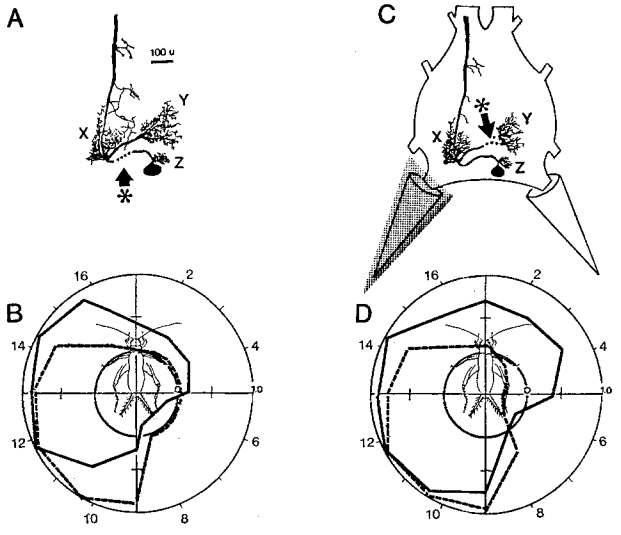

Figure 4. Photoinactivation of identified dendrites. *A* Isolation of dendrite Z. By targeting the laser at the position marked by the arrow, a region indicated by the dotted line in the camera lucida drawing of 10–3 was ablated. Since the recording electrode was in the cell body, only inputs to dendrite Z could be recorded after the ablation. *B* Directional sensitivity recorded before (solid curve) and after (dashed curve) the ablation diagramed in part *A*. Note the loss of inhibition: the dotted line does not dip below the zero line at any point. *C* Ablation of dendrite Y. The laser was targeted at the point marked with an arrow, effectively cutting off all inputs to dendrite Y. The left cercus was covered with vaseline, which blocked all direct excitatory synaptic input onto dendrite X. The only inputs remaining were the synaptic inputs onto dendrite Z (as in case *A* and *B*) and any indirect, polysynaptic inputs onto dendrite X. *D* Directional sensitivity measured from the soma before (solid curve) and after (dashed curve) the ablation diagramed in *C*. The only significant difference in the dashed (i.e. 'after') curves in parts *B* and *D* are the presence of an inhibitory hyperpolarization from regions 2 through 7 in part *D*. (Differences in the 2 'before' curves can be attributed to differences in the angular separation of the two cerci in the two different cases.)

cell body) had been covered with vaseline. This procedure blocks almost all of the wind-evoked excitatory input into the left neuropil. Thus, dendrite 'X' will not receive any direct excitatory input from the sensory afferents. The only dendritic branch receiving direct excitatory afferent input after photoinactivation of dendrite Y is branch 'Z', i.e.: the same as in the laser ablation experiment summarized above. These experiments revealed the contribution of inputs to dendrite Y to the overall receptive field of the neuron. Photoablation of dendrite Y resulted in a loss of excitatory inputs over a specific region of the receptive field. This region coincides with the maximal sensitivity of afferents that overlap with dendrite Y as suggested by the anatomy.

Location of inhibitory inputs revealed by selective lesions

The presumed function of inhibitory inputs in this system is to enhance directional sensitivity by suppressing spontaneous and some wind evoked excitatory inputs[9, 15, 16]. As discussed previously, as well as being excited by wind stimuli from some orientations, the interneurons are inhibited by stimuli from the complementary directions. Maximal inhibition occurs in orientations opposite to orientations of maximal excitation. This can be considered an inhibitory 'surround', in a sense equivalent to the function mediated by lateral inhibition at the horizontal cell layer in the vertebrate retina.

Inhibition is thought to be mediated by local inhibitory interneurons which also receive excitatory input from the filiform afferents[9, 15, 16]. To understand better how this inhibition affects directional selectivity, we determined the stimulus orientations which activated the inhibitory inputs[8]. Inhibitory inputs to interneuron 10–3 could be activated by selected wind stimuli to either cercus. The particular classes of hairs responsible for activating the inhibitory pathway were determined by isolating and stimulating small groups of hairs of known directional sensitivity. Two classes of such hairs were found: one which responded to wind stimuli from the rear of either cercus and another that responded to wind stimuli directed at the lateral face of the cercus ipsilateral to the cell body. Neither of these classes of hairs overlap anatomically with interneuron 10–3, and so must be activating inhibitory interneurons with input dendrites in those regions.

The results of these and other experiments suggest that there may be a non-uniform distribution of inhibitory synaptic inputs onto the dendrites of interneuron 10–3. The location of these inhibitory synapses is of crucial importance to the integration of excitatory inputs. To test this idea the laser ablation technique was used to locate the position of inhibitory inputs in a way similar to that used to locate excitatory inputs. In the experiment in which dendrite Z was isolated from the rest of the neuron (fig. 4A, B) inhibitory inputs disappeared after photoinactivation. These data suggest that very few or none of the inhibitory inputs impinge on dendrite Z. However, when dendrite Y was ablated from the cell (fig. 4C, D) inhibitory inputs visible before the ablation were still effective afterwards.

The location of the spike initiating zone affects integrative properties

The location of the spike initiating zone (SIZ) in a neuron affects the degree to which different excitatory and inhibitory inputs contribute to the spiking output of a cell. The farther a particular input is located from the SIZ, the less will be its contribution to voltage fluctuations at that integrating site. In interneuron 10–3, the relative distances of excitatory or inhibitory inputs to the SIZ could greatly affect their relative contributions to directionally selective spiking output.

Spontaneous and evoked action potentials appear in 10–3's cell body as small (3–5 mV) transients[8, 16]. This implies that the cell body and proximal dendritic membrane are passive, and that the boundary between the passive and active membrane is located at some distance out along the major neurite. In order to determine where the active membrane begins, a series of focal laser ablations were performed. The rationale was that a transection of the dendrite proximal to the active membrane would eliminate action potentials, and that transection of the dendrite distal to the boundary would not eliminate spikes.

In the series of photoablation experiments in which dendrite Z was isolated, all spiking activity in the neuron ceased (fig. 4A, B). Wind stimuli and injected current evoked only smooth depolarizations of the cell. This result indicated that the SIZ was located at or beyond the intersection of dendrite Y with the main neurite. In an attempt to locate the SIZ more precisely, the laser was used to irradiate several spots along the axon (fig. 5A). There were no observable changes in spike amplitude or duration resulting from these irradiations, indicating that the SIZ was proximal to those sites. However, when the cell was illuminated precisely at the site where the axon emerges from dendrite X, there was an immediate (within 1 s) broadening of action potentials followed by loss of action potentials entirely.

We interpret these results to mean that the boundary between active and passive membrane is located at that branch point. Such spike broadening should only be observable

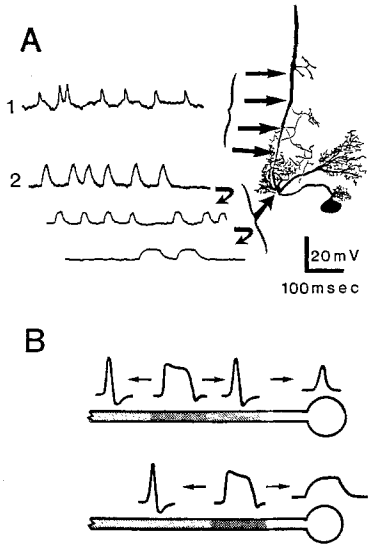

Figure 5. Location of the spike initiating zone (SIZ). *A* Arrows indicate four sites within the region labeled '1' which were photoinactivated after which there were no significant changes in the shapes of action potentials as recorded in the cell body. When the region at position '2' was photoinactivated, there was a rapid broadening of the recorded action potentials. The three traces were recorded 5, 10 and 15 s respectively after the termination of a 3-s laser illumination. *B* Schematic diagram illustrating our hypothesis for these results. The dark cross-hatched areas on the schematic 'neurons' represent membrane with damaged sodium inactivation channels. The light cross-hatched areas represent normal active membrane. The traces above the different areas of cell membrane represent the time course of the voltage transients we would except to observe at the corresponding locations. The spikes at the damaged areas would be very broad, due to the decreased sodium inactivation. (Adapted from Jacobs et al.[9] with permission from The Journal of Neuroscience.)

from a somatic recording site if there were no active membrane in between the site of damage and the recording site. Our reasoning is illustrated in figure 5B. The first observed effect of photoinactivation in active membrane is thought to be a local depolarization and broadening of action potentials, due to the high susceptibility of the sodium inactivation gate to oxidative damage[29]. If this damage is localized to a short segment along an otherwise normal axon, then the undamaged channels on either side of the damaged region would restore the action potential to its normal shape as the spike propagated away from the damaged region. However, if the damage were induced right at the border of active and passive membrane, then the spike shape would not be 'corrected' by the passive membrane, and an attenuated spike would still appear broadened. Hence, this region probably represents the transition between active and passive membrane in the cell. Since this site is also the site of the convergence of all synaptic inputs, it would receive the maximum depolarization from excitatory synaptic inputs. It is therefore likely to be the normal site of spike initiation.

The loaction of the SIZ in interneuron 10–3 is much closer to dendrite X than to either dendrite Y or Z. This suggests that inputs to dendrite X would be more efficacious for spike initiation than inputs to either of the other two dendrites. To test this hypothesis, directional sensitivity was measured two times from the same cell, first with both cerci intact and then with one cercus covered (fig. 6). The number of action potentials at each stimulus orientation was scaled to the control value and plotted on a linear scale according to stimulus orientation. The relative number of spikes produced by inputs onto dendrite X (91%) were far greater than the number produced by inputs onto dendrites Y and Z combined (42%). Note that the directional tuning of the cell was preserved despite the reduction in spike number. Thus dendrite X appears to have a much larger influence on the directionally selective spiking output than either of the other two dendrites. This experiment also illustrates that the summation of synaptic inputs in 10–3 is nonlinear, since the sum of action potentials produced by inputs to each cercus alone is greater than the number produced with both cerci intact. There are two sources of this effect: 1) nonlinearity of summation of excitatory inputs near their reversal potential and 2) coactivation of inhibitory inputs with both cerci intact.

The location of inhibitory inputs with respect to the SIZ could substantially affect the integration of excitatory inputs. Rall has shown by theoretical analysis that the most efficient location for inhibitory synapses would be at a position near the SIZ of the neuron[24]. The laser ablation experiments on interneuron 10–3 suggested that some inhibitory inputs must be located on dendrite X. Inhibitory synapses at this strategic location could limit the spiking output of the cell very effectively since the excitatory synaptic current generated on any of the other dendrites must flow to this region. An inhibitory shunt at that location should prevent the neuron from firing in response to stimuli from several orientations. Thus, relative suppression of excitatory inputs from each individual dendrite need not be achieved by inhibitory synapses located on the dendrite. To suppress excitatory inputs from a particular dendrite, inhibitory inputs located near the SIZ must be coactivated at the same stimulus orientations which evoke excitatory afferent input to that den-

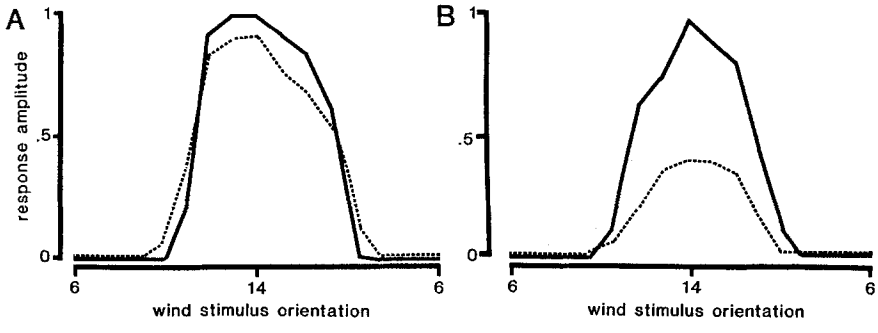

Figure 6. Contribution of inputs onto different dendrites to spiking output in interneuron 10–3. *A* Directional sensitivity of interneuron 10–3 with both cerci intact measured by the number of action potentials generated at each stimulus orientation is shown in the solid line. Dotted line represents the number of action potentials generated by inputs to dendrite X (scaled to the maximum number in the control) after blocking the cercus ipsilateral to the cell body with vaseline. *B* Directional sensitivity of interneuron 10–3 with both cerci intact (solid line) and after blocking the cercus ipsilateral to the axon (dashed line, scaled to the maximum in the control). Dashed line represents the relative contribution of inputs to dendrites Y and Z to the spiking output of the cell. Note that the directional tuning of the cell is very similar when either cercus is stimulated independently.

drite. Thus when the inhibitory directional sensitivity 'matches' the directional sensitivity of excitatory inputs, the relative synaptic efficacy of excitatory inputs onto that dendrite would be selectively decreased.

Conclusion

In the insect nervous system, a great deal is known about the organization of the neuropil into specific sensory, motor and 'association' areas[31]. This knowledge has greatly facilitated studies of the functional roles of identified neurons, since the location of dendrites within particular neuropil regions can be used to predict the types of inputs and output connections a cell could make[1,2,8,33]. These anatomical relationships are of special interest in sensory systems where primary afferents form a 'topographic map' of their receptive fields in the CNS. Sensory interneurons postsynaptic to these afferents interpret these maps by virtue of the position of their dendritic fields within these different neuropil regions.

In the experiments reviewed here, a wind-sensitive interneuron that receives monosynaptic input from filiform hairs was studied. The cellular basis for directional sensitivity in this interneuron was investigated, and three main factors were identified which contribute to its response properties: 1) excitatory inputs from wind sensitive afferents determine the overall excitatory 'receptive field' of the cell (i.e. the wind directions to which the cell is sensitive); 2) inhibitory inputs from other interneurons sharpen the cell's directional sensitivity by suppressing activity for wind directions outside of the excitatory receptive field; and 3) the location of the SIZ determines the relative weighting of inputs onto the different branches thus influencing the cell's directionally selective spiking output.

The laser photoinactivation technique was of crucial importance in these studies. Hypotheses concerning the mechanisms underlying synaptic integration are often formulated in terms of neuronal structure function relationships. These relationships are certainly important in the cercal sensory system, and probably in all other mapped sensory systems as well. However, it has proven very difficult to test such hypotheses definitively, since a truly direct test requires a modification of cell structure during physiological recording. The laser photoinactivation technique is invaluable and perhaps unique in its capability in this respect. The technique continues to be of great value in our studies, and should be applicable in many other systems as well.

1 Bacon, J. P., and Murphey, R. K., Receptive fields of cricket (*Acheta domesticus*) are determined by their dendritic structure. J. Physiol., Lond. *352* (1984) 601.

2 Burrows, M., Parallel processing of proprioceptive signals by spiking local interneurons and motor neurons in the locust. J. Neurosci. *7* (1987) 1064–1080.

3 Edwards, J. S., and Palka, J., The cerci and abdominal giant fibers of the house cricket, *Acheta domesticus*. I. Anatomy and physiology of normal adults. Proc. R. Soc. *185* (1974) 83–103.

4 Gnatzy, W., and Tautz, J., Ultrastructure and mechanical properties of an insect mechanoreceptor: Stimulus transmitting structures and sensory apparatus of the cercal filiform hairs of Gryllus. Cell Tiss. Res. *213* (1980) 441–463.

5 Hubel, D., and Wiesel, T. N., Shape and arrangements of columns in cat's striate cortex. J. Physiol., Lond. *165* (1963) 559–568.

6 Hubel, D., and Wiesel, T. N., Receptive fields and functional architecture of monkey striate cortex. J. Physiol., Lond. *195* (1968) 215–243.

7 Jacobs, G. A., and Miller, J. P., Functional properties of individual neuronal branches isolated in situ by laser photoinactivation. Science *228* (1985) 344–346.

8 Jacobs, G. A., Redfern, C., and Miller, J. P., Identification and characerization of inhibitory inputs in the cricket cercal afferent system. Soc. Neurosci. Abstr. *11* (1985) 164.

9 Jacobs, G. A., Miller, J. P., and Murphey, R. K., Cellular mechanisms underlying directional sensitivity of an identified sensory interneuron. J. Neurosci. *6* (1986) 2298–2311.

10 Jacobs, G. A., and Murphey, R. K., Segmental origins of the cricket giant interneuron system. J. comp. Neurol. *265* (1987) 145–157.

11 Kanou, M., and Shimozawa, T., A threshold analysis of cricket cercal interneurons by an alternating air-current stimulus. J. comp. Physiol. *A 154* (1984) 357–365.

12 Kater, S. B., Cohan, C. S., Jacobs, G. A., and Miller, J. P., Image intensification of stained, functioning and growing neurons, in: Optical Methods in Cell Physiology, vol. 40, pp. 31–50. John Wiley & Sons, New York 1986.

13 Knudsen, E. I., duLac, S., and Esterly, S. D., Computational maps in the brain. A. Rev. Neurosci. *10* (1987) 41–66.

14 Konishi, M., Takahashi, T. T., Wagner, H., Sullivan, W. E., and Carr, C. E., Neurophysiological and anatomical substrates of sound localization in the owl, in: Functions of the Auditory System, (in press) Eds G. M. Edelman and W. E. Gall. John Wiley & Sons, New York 1988.

15 Levine, R. B., and Murphey, R. K., Loss of inhibitory synaptic input to cricket sensory interneurons as a consequence of partial deafferentation. J. Neurophysiol. *43* (1980) 383–394.

16 Levine, R. B., and Murphey, R. K., Pre- and postsynaptic inhibition of identified giant interneurons in the cricket (*Acheta domesticus*) J. comp. Physiol. *135* (1980) 269–282.

17 Matsumoto, S. G., and Murphey, R. K., The cercus-to-giant interneuron system of crickets IV. Patterns of connectivity between receptors and the medial giant interneuron. J. comp. Physiol. *119* (1977) 319–330.

18 Mendenhall, B., and Murphey, R. K., The morphology of cricket giant interneurons. J. Neurobiol. *5* (1974) 565–580.

19 Miller, J. P., and Jacobs, G. A., Relationships between neuronal structure and function. J. exp. Biol. *112* (1984) 129–145.

20 Miller, J. P., and Selverston, A. I., Rapid killing of single neurons by irradiation of intracellularly injected dye. Science *185* (1979) 181–183.

21 Murphey, R. K., The structure and development of a somatotopic map in crickets: The cercal afferent projection. Devl Biol. *88* (1981) 236–246.

22 Murphey, R. K., A second cricket sensory system: bristle hairs and the interneurons they activate. J. comp. Physiol. *A 156* (1985) 357–367.

23 Palka, J., Levine, R., and Schubiger, M., The cercus-to-giant interneuron system of crickets. 1. Some aspects of the sensory cells. J. comp. Physiol. *119* (1977) 267–283.

24 Rall, W., Theoretical significance of dendritic trees for neuronal input-output relations, in: Neural Theory and Modeling, pp. 73–79. Ed. R. F. Reiss. Stanford University Press 1964.

25 Sakaguchi, D. S., and Murphey, R. K., The equilibrium detecting system of the cricket. Physiology and morphology of an identified interneuron. J. comp. Physiol. *150* (1983) 141–152.

26 Selverston, A. I., and Moulins, M. (Eds.), The Crustacean Stomatogastric System. Springer-Verlag, Berlin, Heidelberg 1987.

27 Shimozawa, T., and Kanou, M., Varieties of filiform hairs: range fractionation by sensory afferents and cercal interneurons of a cricket. J. comp. Physiol. *A 155* (1984) 485–493.

28 Shimozawa, T., and Kanou, M., The aerodynamics and sensory physiology of range fractionation in the cercal filiform sensilla of the cricket Gryllus bimaculatus. J. comp. Physiol. *A 155* (1984) 495–505.

29 Spikes, J. D., and Livingston, R., The molecular biology of photodynamic action: sensitized photoautoxidation in biological systems. Adv. radiat. Biol. *3* (1969) 29.

30 Tobias, M., and Murphey, R. K., The response of cercal receptors and identified interneurons in the cricket (*Acheta domesticus*) to air streams. J. comp. Physiol. *129* (1979) 51–59.

31 Tyrer, N. M., and Gregory, G. E., A guide to the neuroanatomy of locust subesophageal and thoracic ganglia. Phil. Trans. R. Soc. *297* (1982) 91–124.

32 Walthall, W. W., and Murphey, R. K., Positional information, compartments and the cercal system of crickets. Devl Biol. *113* (1986) 182–200.

33 Weeks, J. C., and Jacobs, G. A., A reflex behavior mediated by monosynaptic connections between hair afferents and motoneurons in the larval tobacco hornworm, *Manduca sexta*. J. comp. Physiol. *A 160* (1987) 315–329.

0014-4754/88/050362-07$1.50 + 0.20/0